Australian Journal of Basic and Applied Sciences, C(): CC-CC, 2012
ISSN 1991-8178

Using Radiances Of High Spatial Satellite Images To Estimate The Nautical Charts For The River Nile

[1]Abdallah saad, [2]Maher M. Amen, [3]Mervat refaat and [4]Ahmad Morad

[1]Professor of Surveying and Geodesy, Shoubra Faculty of Engineering.
[2]Assoc. Prof. of Surveying, Shoubra Faculty of Engineering.
[3]lecturer. of Surveying, Shoubra Faculty of Engineering.
[4]M.sc. student, Department of Surveying, Shoubra Faculty of Engineering.

Abstract: The importance of river transportation, internationally and locally, is a well-known fact, where, it depends mainly on the efficiency of navigational route, In this research it was proposed to use an alternative method to determine the navigation safe path in the river Nile route with relatively low cost and high speed, by using remote sensing technique, which wasn't used before in the river Nile. For this reason a practical experiment using this technique has been made to prove the possibility of applying it successfully, by using multi-spectral band satellite image with resolution 1.65m, which covers an area of almost 15.52 Km²of the river Nile (of width=1Km and length=15.52Km) from Esna to nagaaHamadii. This study was made on three stages, only for 1Km of the Nile path, at which about 420 data points were available with known geographic position and observed depths with high accuracy. In the first stage, the image was corrected geometrically, by using 7 ground control points, every pixel in the image contains reflected data representing its correct geographic position, but contaminated by errors from some external effects. The second stage concentrates on the removal of these errors, and getting the values of the corrected reflected radiance for every pixel in the image. In the third stage the corrected radiance values were used in a chosen suitable mathematical model, to compute the depths of the Nile bed. At the end these depth values were compared with the observed values. The average of the differences was about (80 Cm). This value is relatively small compared to the route depth of the Nile, therefore it supports and encourages using remote sensing technique, which is easier, cheaper and faster in determining the safe navigational route in the river Nile.

Key words:

INTRODUCTION

The bathymetry is a branch of the hydrographic surveying that deals with the measurement of the depths of the seas and the rivers. Bathymetric information is particularly important in coastal areas which often exhibit a high population density, heavy maritime traffic. In many regions, river depth changes because of erosion and sedimentation processes and bathymetry must often be updated. Bathymetric surveying of the rivers is often performed by conventional ship-based acoustic surveys. However, this technique requires heavy and expensive equipments as well as time consuming data processing .This has encouraged the development of remote sensing based bathymetric techniques. The airborne LIDAR technique, based on laser telemetry, is still very expensive and available on aerial platform only. it can only provide shape location and not quantitative depth.

Multispectral satellite imagery has been used to produce bathymetric maps by considering pixel radiances or reflectance as a depth indicator. This method includes the advantages of the conventional ship-based acoustic survey and the airborne LIDAR technique. This technique has already been applied on different resolution imagery. The fundamental physical principle underlying the retrieval of bathymetric information from optical remote sensing images is that when light passes through water it becomes attenuated by interaction with the water column. Deep areas appear dark on the image since the water absorbs much of the reflected light. Shallow areas appear lighter on the image since less light reflected from the seabed is absorbed in the passage through the water column. Remote sensing was used for bathymetric mapping of coral reefs in the Red Sea (Hurghada – Egypt) as study area, the coral reefs near Hurghada, Egypt, were selected by Landsat7 ETM+ image on September 10th 2000, using depth of penetration (DOP) mapping method, the standard deviation was 2.1m.

This is the first time that the remote sensing bathymetric technique is used for estimating the depths in the river Nile in Egypt. In other locations in the river Nile this technique was achieved successfully to estimate the depths as in Lake Tana, which is the largest lake in Ethiopia and the source of the Blue Nile. Also, this technique succeeded in other rivers around the world as the River Kelantan in Malaysia, Soda Butte Creek in the united states at Wyoming State, Platte River in the United States at Nebraska state and Laramie River in United States at Colorado, Wyoming state.

In this research we used the remote sensing technique for estimating the depths of the river Nile, which were observed by the echo sounder, using geo-eye satellite image through non -linear bathymetric inversion

Corresponding Author: Abdallah saad, Professor of Surveying and Geodesy, Shoubra Faculty of Engineering.

model. The estimated depths were obtained with a relatively low difference versus the traditional depths, with standard deviation (0.460m).

Available Data:

The available data consists of two sets, the first belongs to the traditional technique, and the second refers to the satellite image, in addition to the used software.

3.1. Available Traditional Data From Echo Sounder:

Traditional bathymetric charts are based on individual soundings accumulated during decades of ship-borne surveying operations. Ship-borne surveys with single- beam echo sounders and GPS receivers are applied in the area of Esna bridge. The following results were obtained, The traditional data is checked through empirical field calibration by measuring the depths manually, using a heavy metallic tool at many points, at the beginning of scope , the middle of scope and the end of it during the daily work, also at every stopping and movement of the ship, then comparing these values with those observed by the echo sounder.

Hydrographic surveys use sonar to collect highly accurate water depth and bottom contour information. These echo sounding systems are based on the principle that when a sound signal is sent into the water it will be reflected back when it strikes an object. An instrument, called a transducer, sends a sound pulse straight down into the water. The pulse moves down through the water and bounces off the seafloor. The transducer also picks up the reflected sound. The sonar sensor precisely measures the time it takes for the sound pulse to reach the bottom and return. The water depth is calculated by knowing how fast sound travels in the water.

Sounding data has many confused data because of intercepting of many bodies such as chlorophyll algae and sediments to the waves, so the observed depths should be filtered from wrong value by the hypack software through excluding the observations, which are far away from the average of the observed values (diverged observations), to reach depths that represent the nature of the seabed Nile through the converged observations. As shown in figures below.

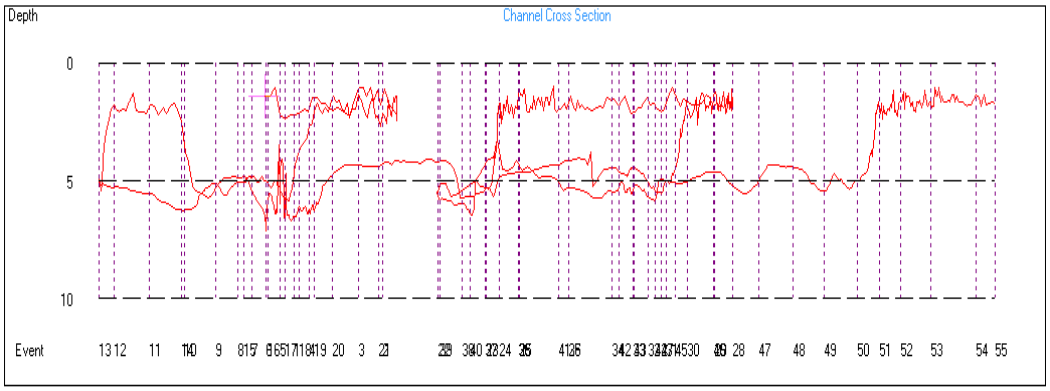

Fig. 1: Traditional technique data without filtration.

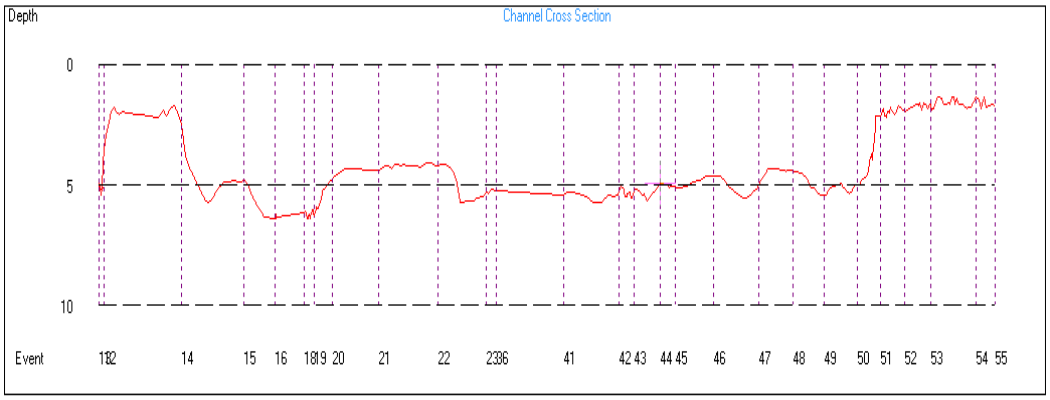

Fig. 2: Traditional technique data was filtered by hypack software.

The following table shows the results of the sample of echo sounder data after filtration.

Table 1: Traditional technique Observations by using GPS and Echo Sounder.

Position by GPS		Traditional Depth by echo-sounder
Easting	Northing	
455173.9	2803257	7.01
455139.4	2803259	6.74
455126.7	2803159	6.55
455090.6	2803158	7.53
455072.4	2803159	6.13
455129.9	2803066	6.07
455180.6	2803063	6.8
455206.8	2802969	6.8
455263.7	2802875	6.98
455243.6	2802876	8.08
455316.6	2802781	8.66
455401.6	2802676	10.61

3.2. Available Satellite Image Data:

A multispectral satellite image with 1.65 m spatial resolution over a chosen area has been selected for this study. This high resolution image was collected in 2009-07-10 08:40 GMT by spacing imaging's GEOEYE satellite and supplied in a TIFF digital format. This image has been obtained and rectified (corrected), the research took the traditional filter data as a guide for filtration of remote sensing data. we depended on 60 points which represent the true nature of the seabed Nile they don't contain any effect of chlorophyll algae, sediments and the shadow of the Nile, but some shift errors still exist, they were removed throw the mathematical models which were presented in the methodology. There were many software packages used for achieving the main aim of this research, such as, Global Mapper12, ERDAS IMAGINE of version 2010, AutoCAD Civil 2011 and GPS data processing program. The study area was chosen at Esna city in El Oqsor governorate as shown in figure below.

Fig. 3: Geoeye Satellite Image.

4. Methodology:

Methodology explained how radiances can be calculated from the pixel values , then correcting the total upwelling radiance (L_t) from the shift errors that affect it, such as atmospheric effect, sun glint effect, subsurface volumetric effect and bottom radiance effect, to extract the corrected radiances, which can be used to compute the depth through the non -linear bathymetric inversion model.

4.1 Converting Satellite Image Pixel Value To Radiance:

Radiometric data processing activity involved in many quantitative applications of digital image data is conversion of DNs to absolute radiance value.
The following equation shows the relation between radiance and DN values for a given channel:

$$L = G * DN + B \quad (1)$$

When:
DN: Digital Number value recorded.
G: slope of response function (channel gain), get it from metadata file.
L: spectral radiance measured (over the spectral bandwidth of the channel).
B: intercept of response function (channel offset) get it from metadata file.

The following table (2) shows computed radiances which are computed from DNs:

Table 2: Obtain false radiances value was computed from digital number for study area samples.

Position by GPS		Traditional Depth by eco-sounder	False Radiance Values	
Easting	Northing		Blue Band	Green Band
455173.9	2803257	7.01	5.853978	4.242270
455139.4	2803259	6.74	5.853978	4.242270
455090.6	2803158	7.53	5.853978	4.242270
455072.4	2803159	6.13	5.853978	4.242270
455110.7	2803066	6.16	5.878995	4.225025
455129.9	2803066	6.07	5.878995	4.225025
455180.6	2803063	6.8	5.828961	4.207780
455206.8	2802969	6.8	5.828961	4.225025
455263.7	2802875	6.98	5.828961	4.207780
455243.6	2802876	8.08	5.828961	4.207780
455316.6	2802781	8.66	5.828961	4.190535
455402	2802676	10.61	5.828961	4.190535

4.2 Total Upwelling Radiance (Lt) Recorded Components:

The total upwelling radiance (L_t) is recorded by the remote sensor. It consists of four components (Figure 1) (Jensen 2007): bottom radiance (L_b), subsurface volumetric radiance (L_v), specular radiance (L_v), and atmospheric path radiance (L_p) as shown in Eq. (2):

$$L_t = L_b + L_v + L_s + L_p \quad (2)$$

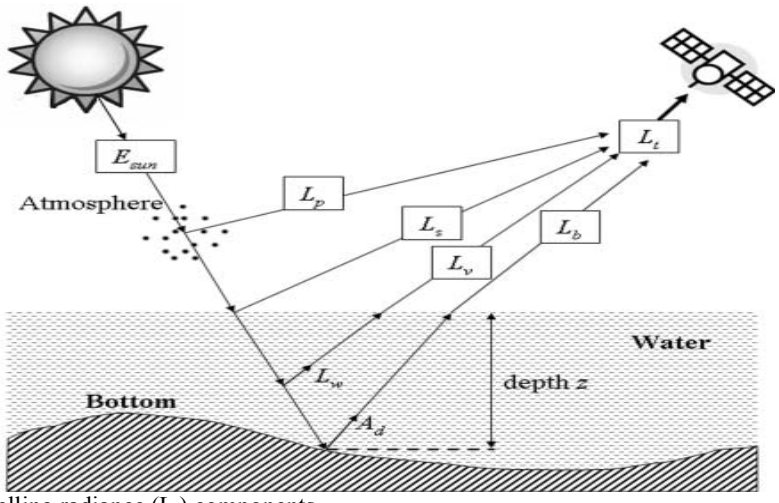

Fig. 4: Total upwelling radiance (L_t) components.

4.2.1 Atmospheric Path Radiance (L_p):

It is a function of atmospheric scattering, including both Rayleigh and Mie scattering.

Using ATCOR model (Atmospheric Correction model) to remove atmospheric effect by some parameters, first the Sun Position, which was calculated from Meta data. Second the following parameters, the sensor tilt, the satellite azimuth and the elevation, which were selected from the library of the geo-eye. Also we import visibility swath width 'km' (15.2 km for geoeye sensor). Finally Aersoltype data from the model library (maritime, midlat_summer_marit). Through these inputs and calculations we get the image corrected from atmospheric effect.

4.2.2 Specular Radiance (L_s):

Sun glint, the specular reflection of light from water surfaces, is a serious confounding factor for remote sensing of water column properties and benthos.

Sun glint occurs in imagery when the water surface orientation is such that the sun is directly reflected towards the sensor and hence, is a function of sea surface state and sun position.

This is based on the assumption that the near infra read (NIR) signal can´t penetrate the water so any NIR signal remained after atmospheric correction must be due to the sun glint.

In our case after applying atmospheric model, the obtained result weren´t corrected from the sun glint, because the sea surface state, sun position and viewing made the NIR radiance equal zero.

4.2.3 Subsurface Volumetric Radiance (L_v):

Subsurface volumetric radiance results from volume scattering from the water and its organic/inorganic constituents (e.g. sediment and chlorophyll). It is closely related to the optical properties of the water column.

$$L_v = -\varepsilon * b * c \quad (3)$$

c: concentration of chlorophyll.
b: water depth.
ε: coefficient constant.

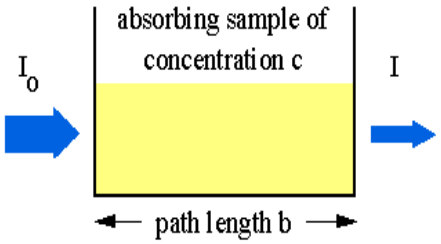

Fig. 5: Obtain volumetric correction elements.

This model explains how to correct the image from subsurface volumetric radiance from chlorophyll concentration only as a factor affect on the image. But in fact there is many factors as sediments and chlorophyll algae affect on the image. These effects don't have a mathematical model to remove it, they are considered as random errors and removed through solving the equations.

4.2.4 Bottom radiance (L_b):

The bottom radiance (L_b) is the energy reflected from the seabed, which integrates the information about water depth and the bottom characteristics (habitat and substrate). To decode water depth information, we need to disaggregate bottom radiance (L_b) from total radiance (L_t).

4.3 Mathematical Model For Computed Depth:

The measured total radiance over optically-deep water ($L\infty$) represents the combined effects of atmospheric path radiance, specular radiance, subsurface volumetric radiance, and the bottom radiance (L_b) **equals zero** for deep water.

After atmospheric and sunglint corrections, the deep water radiance ($L\infty$) only contains subsurface volumetric radiance (L_v).

Assuming that the subsurface volumetric radiance in shallow water is the same as that of adjacent deep water, then optically deep water radiance ($L\infty$) recorded by the remote sensor can be used to correct the subsurface volumetric radiance (L_v) in shallow water.

The following table (3) shows computed radiances which are corrected from last factors effect.

Table 3: Obtain Corrected radiances for study area samples.

Position by GPS		Traditional Depth by eco-sounder	Semi- Corrected Radiances	
Easting	Northing		Blue Band	Green Band
455173.9	2803257	7.01	0.375255	0.310410
455139.4	2803259	6.74	0.375255	0.310410
455126.7	2803159	6.55	0.375255	0.310410
455090.6	2803158	7.53	0.375255	0.310410
455072.4	2803159	6.13	0.400272	0.275920
455129.9	2803066	6.07	0.400272	0.293165
455180.6	2803063	6.8	0.375255	0.310410
455206.8	2802969	6.8	0.375255	0.310410
455263.7	2802875	6.98	0.375255	0.310410
455243.6	2802876	8.08	0.425289	0.310410
455316.6	2802781	8.66	0.350238	0.310410
455401.6	2802676	10.61	0.350238	0.310410

Based on Beer's Law, the intensity of light is attenuated exponentially with depth traveled through the water column, a simple radiative transfer model for optically shallow waters:

$$L = L\infty\,[1 - \exp(-gz)] + A_d \exp(-gz) \quad (4)$$

Where:

$$L = (Lt - L_p - L_s) \quad (5)$$

L: the measured radiance after atmospheric and sunglint corrections,
$L\infty$:the deep water radiance (equivalent to volumetric radiance Lv),
A_d: the upwelling spectral radiance directly reflected from the bottom (before interacting with the overlying water column),
g: a two-way attenuation coefficient
z: the depth.

The second term on the left side of Eq. (5), $A_d \exp(-gz)$, accounts for the attenuation effect of passing through water of depth z, and equals the water leaving bottom radiance (L_b).
The bathymetric inversion model for a single spectral band can be derived from
Eq. (5) as follows:

$$z = g^{-1}\,[\ln(A_d - L\infty) - \ln(L - L\infty)] \quad (6)$$

As shown in Eq. (7), the estimation of depth z from single band measurement L will depend on the determination of A_d and deep water radiance $L\infty$. Assuming that the ratio of bottom reflectance between two spectral bands is constant for all bottom types within a given scene, (Lyzenga 1978; 1981; 1985) derived a bathymetric inversion model for two (and/or multiple) spectral bands as follows:

$$Z = a_0 + \sum_{i=1}^{N} a_i \; ln[L(\lambda_i) - L_\infty(\lambda_i)] \quad (7)$$

Where:
a_i: (i = 0,1, . . . , N) are the constant coefficients
N: the number of spectral bands
$L(\lambda_i)$: the remote sensing radiance after atmospheric and sun glint corrections for spectral band λ_i.
$L\infty(\lambda_i)$: the deepwater radiance for spectral band λ_i. The natural logarithm transformation produces a linear relationship between water depth and deepwater-corrected radiances of spectral bands.
Eq. (8) is referred to as the log-linear inversion (or deepwater correction) model, which has been most widely used for estimating water depths from optical multi-spectral remote sensing imagery.
Recently, (Stumpf *et al*. 2003) proposed a non-linear bathymetric inversion model based on a log-transformed band ratio:

$$Z = m_1 \frac{\ln(nL(\lambda_2))}{\ln(nL(\lambda_1))} - m_0 \ldots\ldots\ldots\ldots\ldots\ldots\ldots (9) \quad (8)$$

Where:

m_0 , m_1, and n: are constant coefficients for the model,
L (λ_1) and L (λ_2): are the remote sensing radiances (after atmospheric and sunglint corrections) for spectral bands λ_1 and λ_2.

By using least square method we can get an estimated depth (Z) by first computing the coefficient (mo, m1, n), with known parameters (observed depth, L (λ2), L (λ1))

-The following table shows the difference between the estimated depths and the traditional depths.

Table 4: Comparing between estimated depths and actual depths.

Position by GPS		Traditional Depth by eco-sounder	Estimated Depth	Difference
Easting	Northing			
455173.9	2803257	7.01	-5.154	1.855
455139.4	2803259	6.74	-5.154	1.585
455126.7	2803159	6.55	-5.154	1.395
455090.6	2803158	7.53	-5.154	2.375
455072.4	2803159	6.13	-8.593	-2.463
455129.9	2803066	6.07	-4.315	1.754
455180.6	2803063	6.8	-5.154	1.645
455206.8	2802969	6.8	-5.154	1.645
455263.7	2802875	6.98	-5.154	1.825
455243.6	2802876	8.08	-6.135	1.944
455316.6	2802781	8.66	-10.226	-1.566
455401.6	2802676	10.61	-10.226	0.383

According to table (4) the differences between the observed depth and the estimated depth ranges from 0.383 m to 2.46 m with mean value of 1.42 m, and standard deviation of 0.460 m for estimated depth and 0.431m for actual depth.

5. Conclusions And Recommendation:

The Following Conclusions Can Summarized As:

- The results in table (4) confirm what have been mentioned in the research, that the new technique saves time and effort. Measuring the depth of the area of study, whose length is 1 Km, it takes only few hours with total cost depends on the cost of getting the satellite image, which differs from a satellite to another one, in addition to a person who do the treatments without dangers opposing the traditional methods.
- With reference to table (3) we will find the effect of removal of the atmosphere, which has great effects on the pixels of the image, it also affects the radiance values, however the other factors have small effect so it can be neglected or removed through the equations, so we advise using the parameters required in the ATCOR model from their sources that were previously pointed to.
-According to the final results of estimated depths shown in table(4) we found that the calculated depths and their standard deviation become nearer to the observed depths and their standard deviation, which prove the success of the second technique in the river Nile.
- The used mathematical model here in this research has proved itself over several other models used for the same purpose.
- While calculating the depths by this technique we should restrict our self not to be close (within 3m) to the banks of the both sides of the river Nile, because the radiance value in this area isn´t real due to the presence of chlorophyll algae, as well as the effect of the shadow on the sides of the river Nile opposing the sun.

REFERENCES

Antoine, D. and A. Morel, 2005. Atmospheric Correction of the MERIS observations. Ove Ocean Case 1 waters.

Benny, A.H. and G.J. Dawson, 1983. Satellite imagery as an aid to bathymetric charting in the Red Sea. The Cartographic Journal, 20: 5-16.

Haibin, S., Li. Hongxing, D. William, 2008. Automated Derivation of Bathymetric Information from Multi-Spectral Satellitde Imagery Using a Non-Linear Inversion Model. Marine Geodesy, 31: 281-298.

Jupp, D.L.B., 1988. Background and extensions to depth of penetration (DOP) mapping in shallow coastal waters. Proceedings of the Symposium on Remote Sensing of the Coastal Zone, Gold Coast, Queensland.

Lyzenga, D.R., 1978. Passive remote sensing techniques for mapping water depth and bottom features Applied Optics., 17: 379-383.

Lyzenga, D.R., 1985. Shallow-water bathymetry using combined lidar and passive multispectral scanner data. International Journal of Remote Sensing, 6:115-125.

Richard, K., Arledge Ervin B. Hatcher, 2008. Investigating The Effects Of Higher Spatial Resolution On Benthic Classification Accuracy At Midway Atoll , September

Ron Abileah jOmegak San Carlos, 2002. CA 94070 "mapping shallow water depth from satellite"IKONOS satellite.

Stumpf, R.P., K. Holderied and M. Sinclair, 2003. Determination of water depth with high-resolution satellite imagery over variable bottom types. Limnology and Oceanography, 48: 547-556.

Tony, V., G. Rudi, K. Tharwat, 2003. Remote sensing as a tool for bathymetric mapping of coral reefs in the Red Sea (Hurghada – Egypt).